Supplementary Information

HDAC Inhibitors Induce Apoptosis in Myeloid Leukemia by Suppressing Autophagy.
Stankov et al. 2013

Supplementary Materials and Methods

Autophagy manipulation. Autophagy manipulation was performed in accordance to the recently updated guidelines.[1] Activation was achieved using rapamycin, PP242 (0.5-5μM) or starvation (Hank's Buffered Salt Solution [HBSS] supplemented with 6mM glucose). Inhibition of autophagy was achieved as follows: autophagosome-lysosome fusion using vinblastine and nocodazole (12 to 50μM); autophagolysosomal degradation using NH_4Cl (10 to 20mM), chloroquine and hydroxychloroquine (5 to 100μM)[1] All substances were obtained from Sigma Aldrich.

Constructs, retroviral infection and electroporation. pBABEpuro GFP-LC3 (plasmid 22405) and pBABE-puro mCherry-EGFP-LC3B (plasmid 22418) generated by Dr. Debnath[2] were purchased from Addgene. The GFP-LC3 and mCherry-EGFP-LC3B sequences (available at http://www.addgene.org/pgvec1) were introduced into retroviral constructs for subsequent cell transduction. shTP53-sense and -antisense oligonucleotides (Qiagen; sequence available upon request) were cloned into the pRRL-YELLOW lentiviral expression vector. shHDAC1 (V2LHS_61808) and shHDAC2 (V2LHS_132136; Openbiosystems) were cloned into a modified pLEGO-Cerulean expression vector.[3] Retroviral and lentiviral production, cell transduction and selection were performed as described.[4,5] Cells ($1x10^6$) were electroporated (330 V, 10 ms) in 100 μL medium containing 0.5 μg siRNAs (ON-TARGETplus SMARTpool, Dharmacon) directed against *HDAC1, HDAC2, ATG5* or *ATG7* in a 4 mm electroporation cuvette using an EPI 2500 gene pulser (Fischer).

Autophagy measurement. Autophagic activity was measured in accordance to the recently updated guidelines.[1] The following antibodies were used for Western blot analysis: donkey anti-goat Ig-HRP (Santa Cruz), LC-3B and ACTB (both Sigma-Aldrich). Fluorescence microscopy analysis of autophagic punctae was performed using mCherry-LC3-GFP transgenic expression.[1] Flow cytometric analysis of autophagic flux was measured as changes in total cellular LC3-GFP as previously described.[6] Autophagic flux was also assessed as accumulation of total cellular LC3-GFP signal after the addition of CQ. ΔMFI LC3-GFP = MFI LC3-GFP (+CQ) - MFI LC3-GFP (-CQ).[1] Alternative detection of autophagic flux (turnover) was performed using Cyto-ID® Autophagy Detection Kit (Enzo Life Sciences) according to manufacturer's instructions.[7] Autophagic flux (ΔMFI Cyto-ID) is measured as accumulation of autophagic compartments (total cellular Cyto-ID signal) after blockage of autophagolysosomal degradation through elevation/neutralization of lysosomal pH using lysosomotropic compounds CQ or NH_4Cl. ΔMFI Cyto-ID = MFI Cyto-ID (+CQ/NH_4Cl) - MFI Cyto-ID (-CQ/NH_4Cl).

Western blots and immunoprecipitation (IP). Cell lysates were prepared and Western blot analyses and immunoprecipitation were performed as described previously.[8,9] The following antibodies were used: Histone H3 (clone A3S), acetyl-histone-H3, histone H4 (clone 62-141-13), acetyl-histone-H4, phospho-histone H2A.X (Ser139; clone JBW301), (all Millipore), HDAC1, HDAC2 (all Cell Signaling), ATG5, ATG7, anti-mouse IgG HRP and anti-rabbit IgG HRP (all Santa Cruz).

Quantitative real-time PCR (qRT-PCR). RNA isolation, cDNA synthesis and qRT-PCR were performed as previously described.[8] Analysis was done on a StepOnePlus

(Applied Biosystems) or an iCycler (Bio-Rad). qRT-PCR primers are available upon request.

Cell death, apoptosis and proliferation assays. Cycle analysis using the BrdU Flow Kit and apoptosis analyses using the Annexin V Apoptosis Detection Kit II were performed according to manufacturer's instructions (BD Pharmingen) and as previously described.[8,10] Alternatively, apoptosis and cell cycle were measured by propidium iodide (PI) nuclear staining or by changes of cellular FSC vs SSC dot plot as previously described.[9,11,12] Cell death was measured by PI exclusion assay. Proliferation was measured by cell counts and CFSE dilution method.[13] The Caspase 3/7 activity assay was performed using the Caspase-Glo® 3/7 Assay Systems (Promega) according to the manufacturer's instructions. Total mitochondrial pool was measured using MitoTracker Green (Invitrogen) and ROS using CM-H_2DCFDA (Invitrogen) according to manufacturer's protocol and as previously described.[6,14] Measurements were performed on a Cytomics FC 500, NAVIOS (Beckman Coulter) or LSR II (Becton Dickinson, Biosciences).

Cellular Respiratory Assays. Oxygen consumption rate (OCR) of cells was assessed by using XF24 extracellular flux analyzer (Seahorse Bioscience). After coating with 0.01% poly-L-lysine (Sigma), 6 x 10^5 cells per well were seeded in custom 24-well plates 14-24h before metabolic flux analysis. One hour before starting the assay, growth media was changed to DMEM (with 6mM Glucose) and incubated at 37°C without CO_2. During the assay, four inhibitors of mitochondrial function were sequentially injected, namely oligomycin 2.5µM, FCCP 0.4µM, rotenone 0.1µM and antimycin A 0.1µM. Measurements are reported in pmol/min for OCR. ATP content was measured using

CellTiter-Glo® Luminescent Cell Viability Assay (Promega) according to the manufacturer's instructions after addition of glycolysis inhibitor 2-deoxy-D-glucose (2-DG; Sigma) and oligomycin.

Supplementary Figures

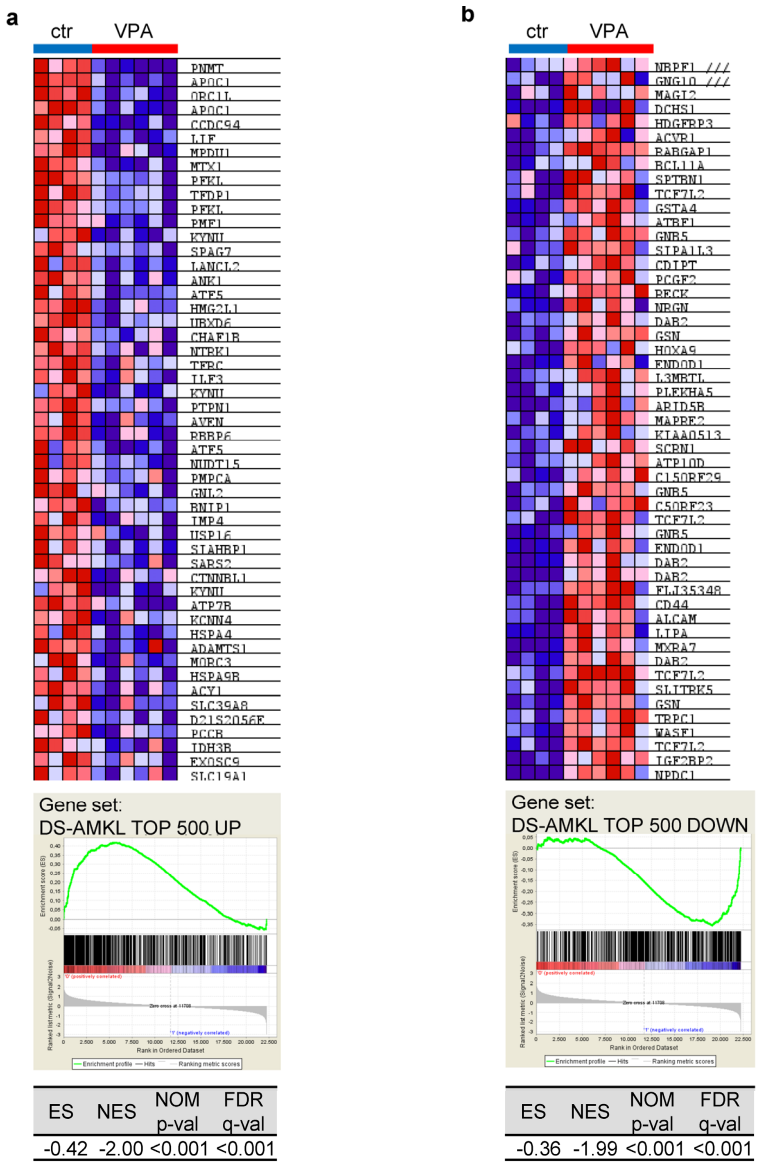

Supplementary Figure 1. VPA represses the DS-AMKL gene expression signature. GSEA of CMY and CMK cells with (VPA) or without (ctr) VPA treatment using the top 500 (a) up- and (b) downregulated genes in DS-AMKL.[15] GSEA indicated the repression of (a) the top 500 upregulated genes and activation of (b) the top 500 downregulated genes by VPA suggesting an inversion of the DS-AMKL gene signature. Cells were treated with 1mM (for 24h and 48h) or 2mM VPA (for 24h). Top - heat maps (top 50 genes are shown). Bottom - enrichment plots and statistics.

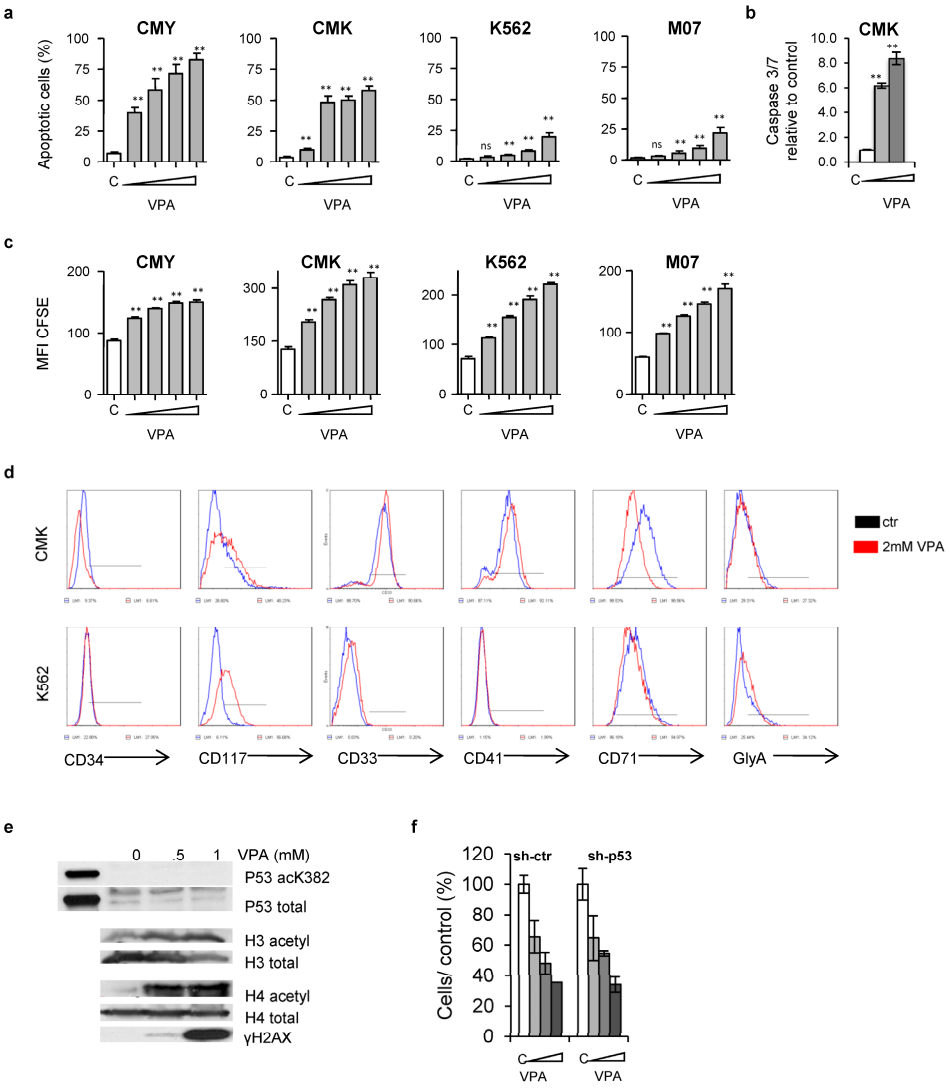

Supplementary Figure 2. VPA induces apoptosis and cell cycle arrest in DS-AMKL cell lines.

(a) Percentage of apoptotic cells assessed by nuclear staining of CMY, CMK, K562 and M07 cells after 24h treatment with increasing doses of VPA (1, 2, 5 and 10mM) compared to control (C).

(b) Caspase 3/7 activity relative to the untreated control 48h after VPA treatment (1 and 2mM).

(c) Diagrams showing proliferation-associated dilution of CFSE determined by decrease in MFI of CMY, CMK, K562 and M07 cells 48h after treatment with increasing doses of VPA (1, 2, 5 and 10mM) compared to lowest MFI (=maximal proliferation) of untreated control cells (C). (a-c) All experiments are presented as mean±s.d. and are representative for at least three independent experiments with three to eight replicates. *P<0.05; **P<0.01.

(d) Flow cytometric analysis of CMK and K562 cells with (red line) or without (blue line) incubation with 2mM VPA for 48h using the indicated antibodies.

(e) Western blot analysis of CMK cells 24h after treatment with the indicated concentrations of VPA using the indicated antibodies.

(f) Number of CMK cells transduced with *shTP53* (*sh-p53*) or the empty vector control (*sh-ctr*) 48h after treatment with increasing doses of VPA (0.5, 1, 2mM) relative to the untreated control (100%) presented as mean±s.d.

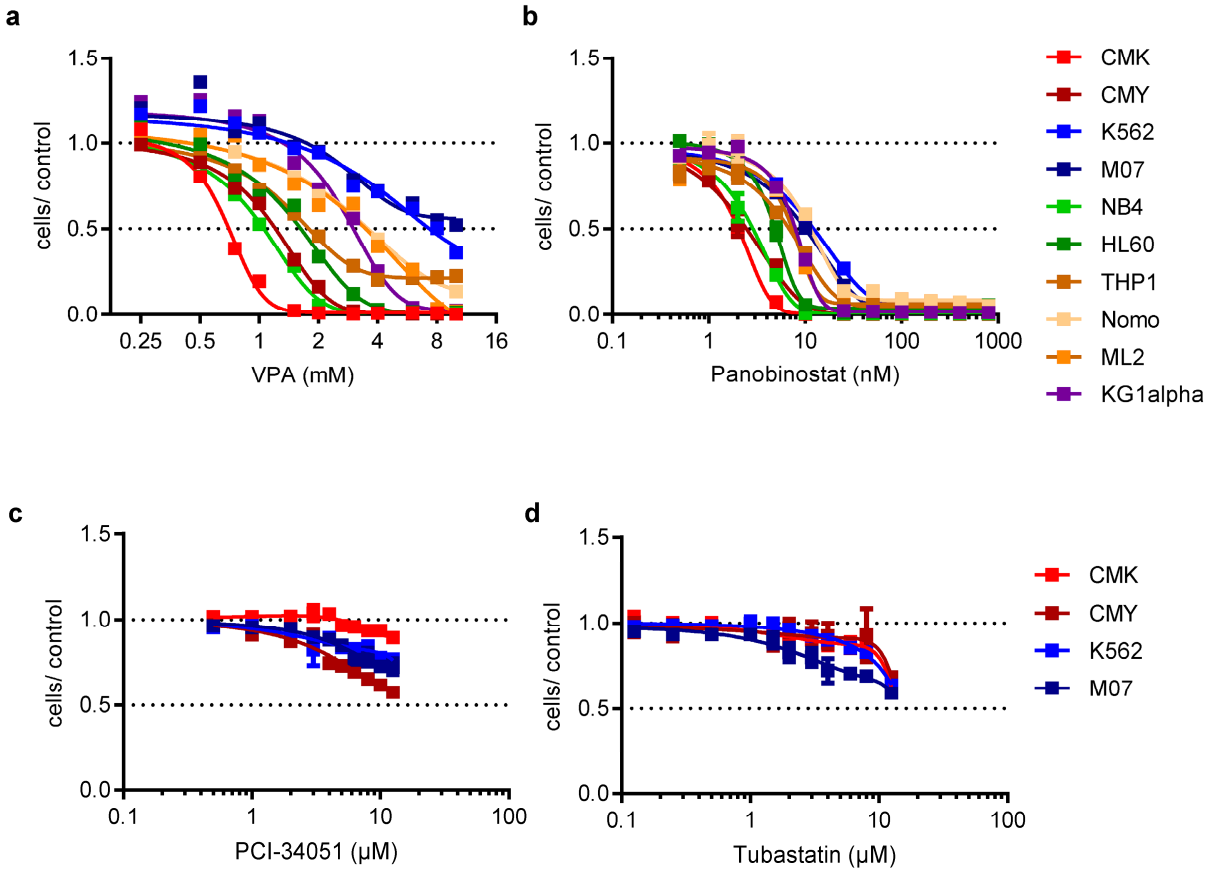

Supplementary Figure 3. Sensitivity of AML cell lines against HDACis.
(a-d) Percent of viable cells 48h after incubation with the indicated concentrations of (a) VPA, (b) Panobinostat, (c) PCI-34051 and (d) Tubastatin in relation to the control. Data are represented as mean±s.d. from replicates from two independent experiments.

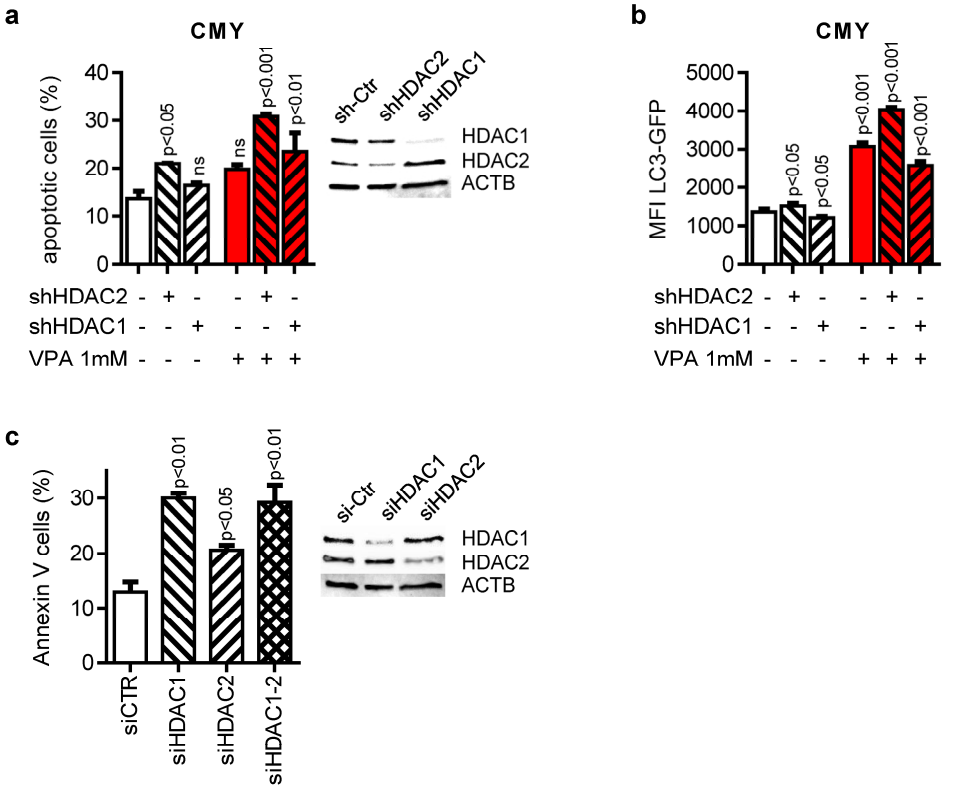

Supplementary Figure 4. shRNA- or siRNA-mediated knockdown of HDAC1 or HDAC2 in CMY cells.

(a-b) Diagrams showing the (a) percentage of apoptotic cells (left) and the knockdown confirmed by western blotting (right) and (b) autophagic flux (LC3-GFP; MFI±s.d.) analyzed by flow cytometry of CMY cells 96h after selection of *shHDAC1, shHDAC2* or the empty vector control transduced cells and 48h after addition of VPA (1mM). Data are representative for at least three independent experiments with two to eight replicates. (c) Diagram showing the percentage of Annexin V^+ cells (left) and the knockdown confirmed by western blotting (right) analyzed by flow cytometry of CMY cells 48h after transfection with *siHDAC1, siHDAC2* or non-silencing control siRNA (siCTR). Data are representative for replicates of two independent experiments.

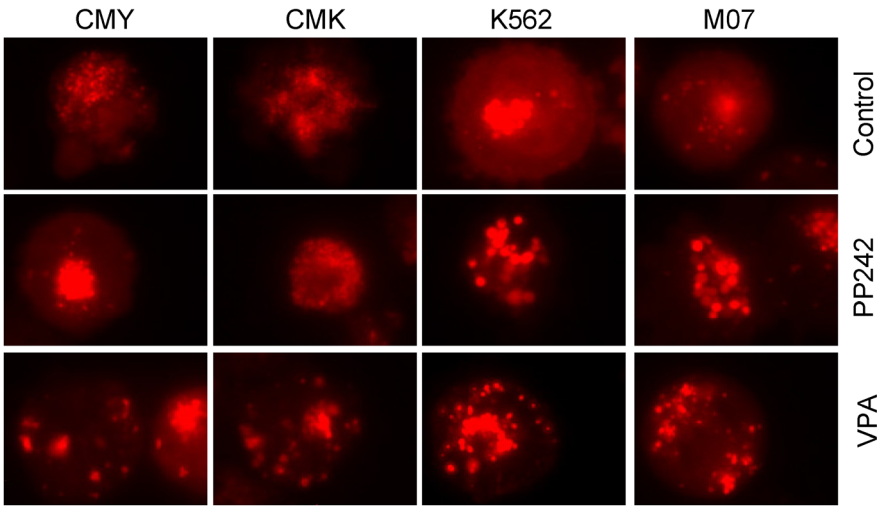

Supplementary Figure 5. Induction of autophagy after VPA Treatment
Fluorescence microscope images representing the formation of autophagic punctae in CMY, CMK, K562 and M07 cells expressing LC3-mCherry in the presence or absence of PP242 (5μM) or VPA (2mM) treatment for 4h.

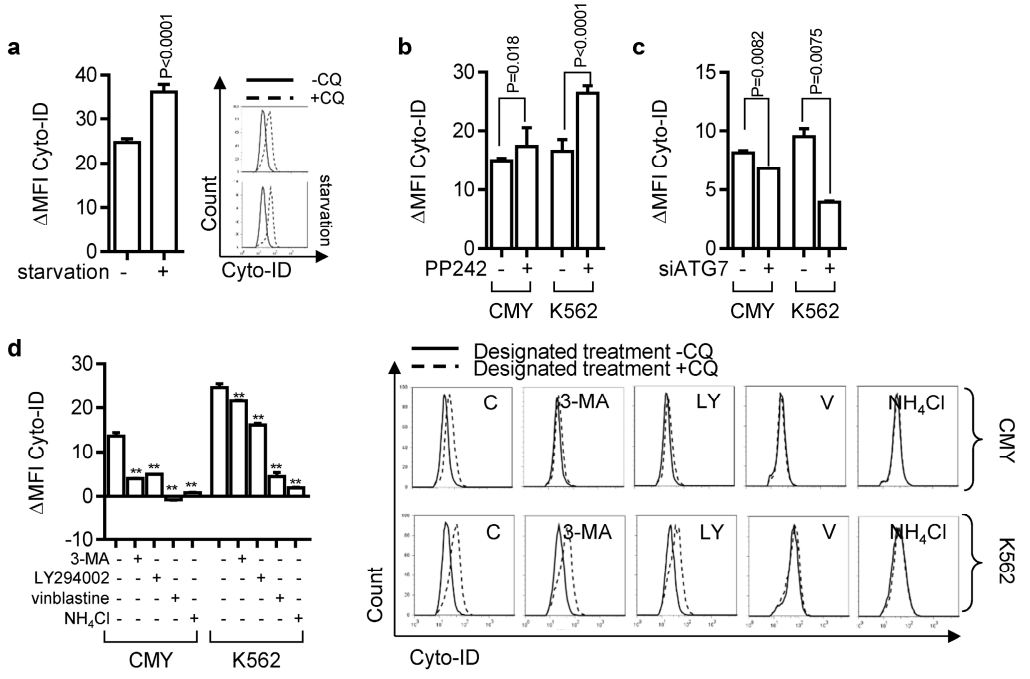

Supplementary Figure 6. Flow cytometry analysis of autophagic flux using Cyto-ID® Autophagy Detection Kit.

Autophagic flux was assessed as accumulation of autophagic compartments (pre-autophagosomes, autophagosomes, and autophagolysosomes) after addition of late autophagic inhibitors NH_4Cl or chloroquine (CQ) for the last 5h measured by changes in total cellular Cyto-ID® signal (ΔMFI Cyto-ID).

(a) Flow cytometry analysis of basic and HBSS activated autophagic flux in K562 cells (left) and representative histograms (right).

(b) Basic and PP242 activated autophagic flux in CMY and K562 cells.

(c) Basic autophagic flux in CMY and K562 cells after siRNA mediated knockdown of ATG7.

(d) Basic autophagic flux in CMY and K562 cells pre-treated with autophagy inhibitors 3-MA (10mM), LY294002 (20μM), vinblastine (V) (12μM) and NH_4Cl (20mM) (left) and representative histograms (right).

(a-d) experiments are presented as mean±s.d. and are representative for at least three independent experiments with two to six replicates. (a-c) *$P_{T\text{-}Test}$<0.05; **$P_{T\text{-}Test}$<0.01. (D) *P_{ANOVA}<0.05; **P_{ANOVA}<0.01.

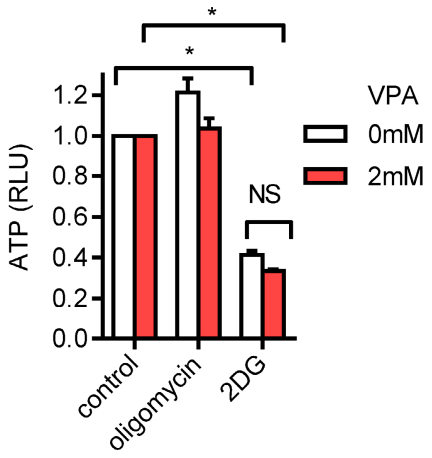

Supplementary Figure 7. Effect of VPA on ATP production
Cellular ATP levels assessed by luminescent assay after addition of glycolysis inhibitor 2-deoxy-D-glucose (2-DG) and the mitochondrial uncoupler oligomycin (inhibitor of mitochondrial complex V; Fig. 4e) in relation to the untreated control with or without addition of VPA. Equal numbers of cells were assessed. *P<0.05.

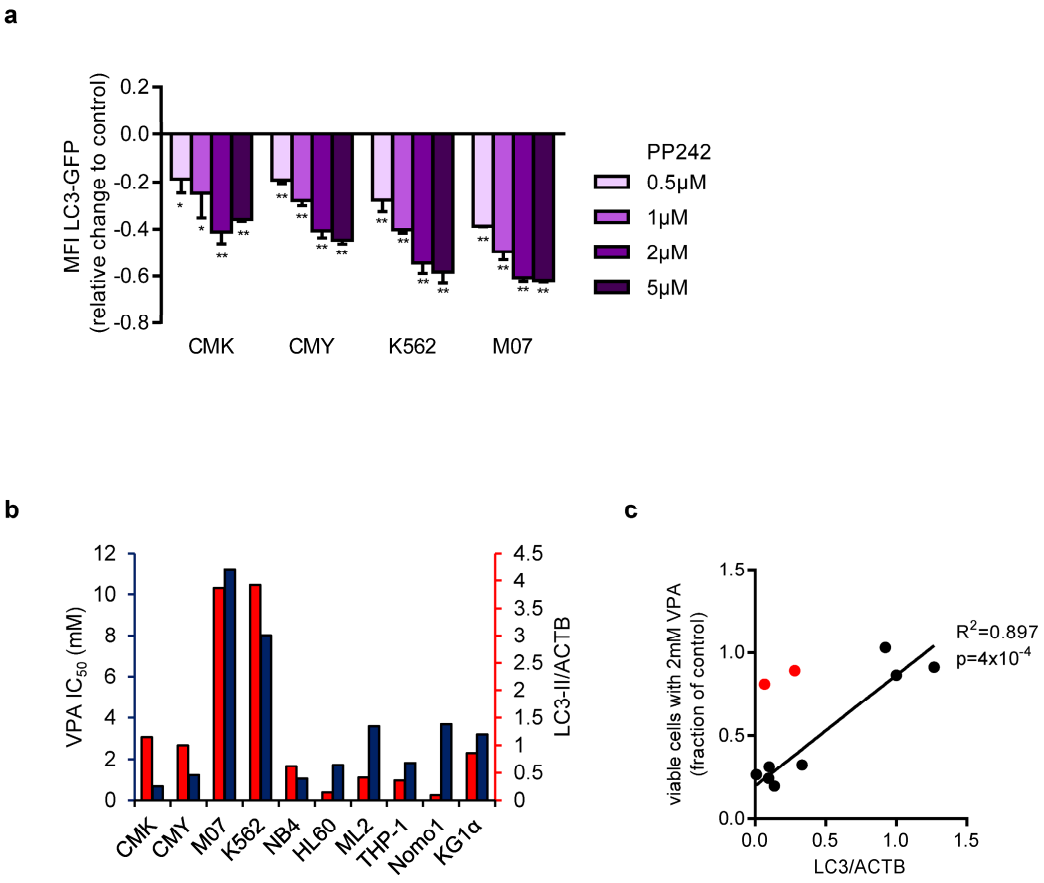

Supplementary Figure 8. Basal autophagy level predicts sensitivity against HDACi
(a) Flow cytometric analysis of CMY, CMK, K562 and M07 cells expressing LC3-GFP after incubation with PP242 (0.5, 1, 2, 5μM) for 17h. The mean fluorescence intensity (MFI)±s.d. in relation to the untreated control (=0) is presented.(b) Diagram showing the level of LC3-II normalized to ACTB assessed by densitometry (blue bars and blue Y-axis) and the IC_{50} to VPA (red bars and red Y-axis) from the indicated cell lines. Viability was determined for cells grown in liquid culture for 48h after addition of 2mM VPA in relation to the untreated control (100%).(c) X-Y-Diagram showing the correlation of LC3-II normalized to ACTB (X-axis) and the fraction of viable cells determined by luminescent cell viability assay (Y-axis) from patients with AML FAB M4eo (n=2), AML with MLL rearrangement (n=2), AML FAB M3 (n=2), AML FAB M2 (n=2; red), AML FAB M7 (or non-DS-AMKL; n=1) and in CD34+HSPCs (n=1) samples (48h after 2mM VPA).

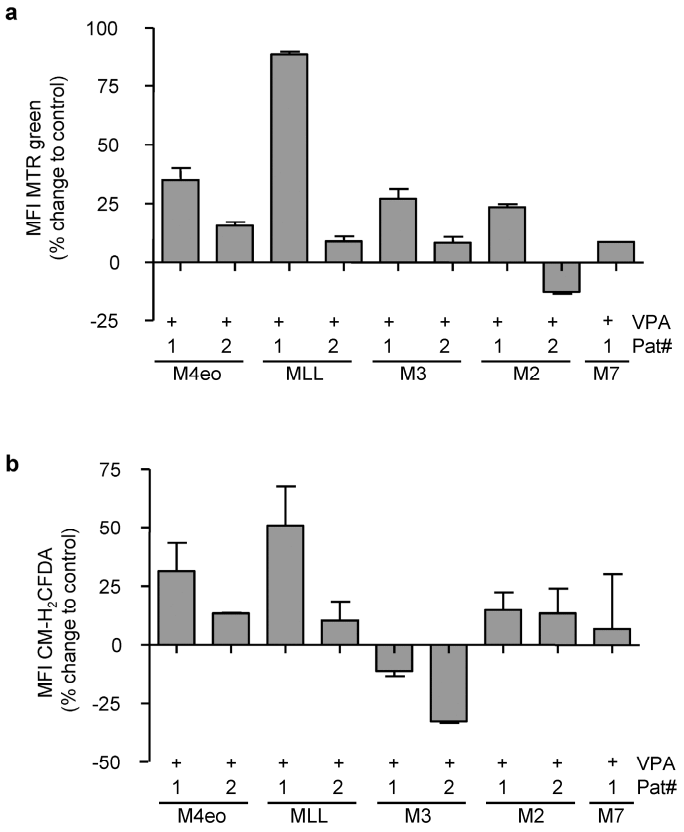

Supplementary Figure 9. VPA leads to the accumulation of mitochondria and to an increased level of ROS in primary leukemic blasts.
(a) Diagram showing the mitochondrial pool analyzed by flow cytometry (MFI±s.d.) of MitoTracker Green (MTR)-stained blasts from patients with AML FAB M4eo (n=2), AML with MLL rearrangement (n=2), AML FAB M3 (n=2), AML FAB M2 (n=2), AML FAB M7 (or non-DS-AMKL; n=1) treated with 10mM VPA relative to the untreated control (0%).
(b) Diagram showing the ROS production analyzed by flow cytometry (MFI ±s.d.) of CM-H_2DCFDA treated leukemic blasts treated with 10mM VPA relative to the untreated control (0%).
Experiments are presented as mean±s.d. and are representative for at least three independent experiments with two replicates.

Supplementary Tables

Supplementary Table 1. Inhibitory selectivity[16-20] of HDAC inhibitors used.

	HDAC class I				HDAC class IIb		DS-AMKL	
Inhibitor Name	HDAC1	HDAC2	HDAC3	HDAC8	HDAC6	HDAC10	sensitivity	Ref.
VPA (mM)	1.6	3.1	3.1	7.4	>10	nd	+	16
	0.7	1	9.4	12.7	>20	>20		17
TSA (nM)	2	3	4	456	3	nd	+	16
	10	12	41	>1000	109	>1000		17
	0.2	0.65	0.5	45	1	nd		18
Panobinostat (nM)	3	3	4	248	61	nd	+	16
	1	0.65	1.1	105	1.5	nd		18
MS-275 (nM)	181	1155	2311	>10000	>10000	nd	+	16
	22	65	360	-	-	nd		18
SAHA (µM)	0.07	0.16	0.05	1.52	90	nd	+	16
	0.28	0.35	0.29	>10	0.13	5.26		17
	0.0013	0.0016	0.005	0.48	0.0016	nd		18
Apicidin (nM)	>10000	120	43	575	>10000	nd	+	16
	40	120	260	49	-	nd		18
PCI-34051 (µM)	4	>50	>50	0.01	2.9	13	-	20
Tubastatin A HCl (µM)	16.4	>30	>30	0.854	0.015	>30	-	19

Half maximal inhibitory concentrations (IC50s)[16,19,20] needed to inhibit the activities of the indicated deacetylases in vitro, the dissociation constants (K_d^{app})[17] or the inhibitory potency (K_i)[18] are provided. Blue text color indicates insensitivity, red color sensitivity.

Supplementary References

1. Mizushima,N., Yoshimori,T. & Levine,B. Methods in mammalian autophagy research. *Cell* **140**, 313-326 (2010).

2. Fung,C., Lock,R., Gao,S., Salas,E. & Debnath,J. Induction of autophagy during extracellular matrix detachment promotes cell survival. *Mol. Biol. Cell* **19**, 797-806 (2008).

3. Weber,K., Bartsch,U., Stocking,C. & Fehse,B. A multicolor panel of novel lentiviral "gene ontology" (LeGO) vectors for functional gene analysis. *Mol. Ther.* **16**, 698-706 (2008).

4. Diessenbacher,P. *et al.* NF-kappaB inhibition reveals differential mechanisms of TNF versus TRAIL-induced apoptosis upstream or at the level of caspase-8 activation independent of cIAP2. *J. Invest Dermatol.* **128**, 1134-1147 (2008).

5. Emmrich,S. *et al.* miRNAs can increase the efficiency of ex vivo platelet generation. *Ann. Hematol.* **91**, 1673-1684 (2012).

6. Stankov,M.V. *et al.* Autophagy inhibition due to thymidine analogues as novel mechanism leading to hepatocyte dysfunction and lipid accumulation. *AIDS* **26**, 1995-2006 (2012).

7. Chan,L.L. *et al.* A novel image-based cytometry method for autophagy detection in living cells. *Autophagy.* **8**, 1371-1382 (2012).

8. Klusmann,J.H. *et al.* miR-125b-2 is a potential oncomiR on human chromosome 21 in megakaryoblastic leukemia. *Genes Dev.* **24**, 478-490 (2010).

9. Kavuri,S.M. *et al.* Cellular FLICE-inhibitory protein (cFLIP) isoforms block CD95- and TRAIL death receptor-induced gene induction irrespective of processing of caspase-8 or cFLIP in the death-inducing signaling complex. *J. Biol. Chem.* **286**, 16631-16646 (2011).

10. Klusmann,J.H. *et al.* Developmental stage-specific interplay of GATA1 and IGF signaling in fetal megakaryopoiesis and leukemogenesis. *Genes Dev.* **24**, 1659-1672 (2010).

11. Williams,O. Flow cytometry-based methods for apoptosis detection in lymphoid cells. *Methods Mol. Biol.* **282**, 31-42 (2004).

12. Janes,M.R. *et al.* Effective and selective targeting of leukemia cells using a TORC1/2 kinase inhibitor. *Nat. Med.* **16**, 205-213 (2010).

13. Constabel,H., Stankov,M.V., Hartwig,C., Tschernig,T. & Behrens,G.M. Impaired lung dendritic cell migration and T cell stimulation induced by immunostimulatory oligonucleotides contribute to reduced allergic airway inflammation. *J. Immunol.* **183**, 3443-3453 (2009).

14. Stankov,M.V., Lucke,T., Das,A.M., Schmidt,R.E. & Behrens,G.M. Mitochondrial DNA depletion and respiratory chain activity in primary human subcutaneous adipocytes treated with nucleoside analogue reverse transcriptase inhibitors. *Antimicrob. Agents Chemother.* **54**, 280-287 (2010).

15. Bourquin,J.P. *et al.* Identification of distinct molecular phenotypes in acute megakaryoblastic leukemia by gene expression profiling. *Proc. Natl. Acad. Sci. U. S. A* **103**, 3339-3344 (2006).

16. Khan,N. *et al.* Determination of the class and isoform selectivity of small-molecule histone deacetylase inhibitors. *Biochem. J.* **409**, 581-589 (2008).

17. Bantscheff,M. & Drewes,G. Chemoproteomic approaches to drug target identification and drug profiling. *Bioorg. Med. Chem.* **20**, 1973-1978 (2012).

18. Bradner,J.E. *et al.* Chemical phylogenetics of histone deacetylases. *Nat. Chem. Biol.* **6**, 238-243 (2010).

19. Butler,K.V. *et al.* Rational design and simple chemistry yield a superior, neuroprotective HDAC6 inhibitor, tubastatin A. *J. Am. Chem. Soc.* **132**, 10842-10846 (2010).

20. Balasubramanian,S. *et al.* A novel histone deacetylase 8 (HDAC8)-specific inhibitor PCI-34051 induces apoptosis in T-cell lymphomas. *Leukemia* **22**, 1026-1034 (2008).